

# Low Loss (~6.45dB/cm) Sub-Micron Polycrystalline Silicon Waveguide Integrated with Efficient SiON Waveguide Coupler

Q. Fang<sup>1</sup>, J. F. Song<sup>1,2</sup>, S. H. Tao<sup>1</sup>, M. B. Yu<sup>1</sup>, G. Q. Lo<sup>1</sup>, and D. L. Kwong<sup>1</sup>

<sup>1</sup>Institute of Microelectronics, A\*STAR, 11Science Park Road, Science Park II, Singapore 117685  
<sup>2</sup>State Key Laboratory on Integrated opto-electronics, College of Electronic Science and Engineering, Jilin University, Changchun, People's Republic of China, 130023  
[Fangq@ime.a-star.edu.sg](mailto:Fangq@ime.a-star.edu.sg)

**Abstract:** In this communication, the sub-micron size polycrystalline silicon (poly-Si) single mode waveguides are fabricated and integrated with SiON waveguide coupler by deep UV lithography. The propagation loss of poly-Si waveguide and coupling loss with optical flat polarization-maintaining fiber (PMF) are measured. For whole C-band (i.e.,  $\lambda \sim 1520\text{-}1565\text{nm}$ ), the propagation loss of TE mode is measured to  $\sim 6.45 \pm 0.3\text{dB/cm}$ . The coupling loss with optical flat PMF is  $\sim 3.4\text{dB/facet}$  for TE mode. To the best of our knowledge, the propagation loss is among the best reported results. This communication discusses the factors reducing the propagation loss, especially the effect of the refractive index contrast. Compared to the SiO<sub>2</sub> cladding, poly-Si waveguide with SiON cladding exhibits lower propagation loss.

©2007 Optical Society of America

**OCIS Codes:** (130.3120) Integrated optics devices; (130.2790) Guided waves; (220.0220) Optical design and fabrication; (220.4000) Microstructure fabrication; (230.3990) Microstructure devices

---

## References and links

1. R. A. Soref and J. P. Lorenzo, "All-Silicon Active and Passive Guided-Wave Components for  $\lambda = 1.3$  and  $1.6\mu\text{m}$ ," *IEEE J. Quantum Electron.* **22**, 873-879 (1986).
2. P. Kyle, S. Bradley, and L. Michal, "Polysilicon Photonic Resonators for Large-Scale 3D Integration of Optical Networks," *Opt. Express* **15**, 17283-17290 (2007).
3. L. Liao, D. Samara-Rubio, M. Morse, A. Liu, D. Hodge, D. Rubin, U. D. Keil, and T. Franck, "High Speed Silicon Mach-Zehnder Modulator," *Opt. Express* **13**, 3129-3135 (2005).
4. A. Liu, R. Jones, L. Liao, D. Samara-Rubio, D. Rubin, O. Cohen, R. Nicolaescu, and M. Paniccia, "A High-Speed Silicon Optical Modulator based on a Metal-Oxide-Semiconductor Capacitor," *Nature* **427**, 615-618 (2004).
5. A. Liu, L. Liao, D. Rubin, H. Nguyen, B. Ciftcioglu, Y. Chetrit, N. Izhaky, and M. Paniccia, "High-Speed Optical Modulation based on Carrier Depletion in a Silicon Waveguide," *Opt. Express* **15**, 660-668 (2007).
6. P. T. Liu and H. H. Wu, "High-Performance Polycrystalline-Silicon TFT by Heat-Retaining enhanced Lateral Crystallization," *IEEE Electron Device Lett.* **28**, 722-724 (2007).
7. S. C. Chen, T. C. Chang, P. T. Liu, Y. C. Wu, J. Y. Chin, P. H. Yeh, L. W. Feng, and C. H. Lien, "Nonvolatile Si/SiO<sub>2</sub>/SiN/SiO<sub>2</sub>/Si type Polycrystalline Silicon Thin-Film-Transistor Memory with nanowire channels for improvement of erasing characteristics," *Appl. Phys. Lett.* **91**, 1903103 (2007).
8. K. C. Moon, J. H. Lee and M. K. Han, "The study of hot-carrier stress on Poly-Si TFT employing C-V measurement," *IEEE Trans. Electron Devices* **52**, 512-517 (2005).
9. A. Harke, M. Krause, and J. Mueller, "Low-loss single mode Amorphous Silicon Waveguides," *Electron. Lett.* **41**, 1377-1379 (2005).
10. L. Sirleto, M. Iodice, C. Della, *et al.*, "Digital optical switch based on Amorphous Silicon Waveguide," *Opt. Lasers Eng.* **45**, 458-462 (2007).
11. R. Sun, P. Dong, N. N. Feng, C. Y. Hong, J. Michel, M. Lipson, and L. Kimerling, "Horizontal, single, and multiple slot waveguides optical transmission at  $\lambda = 1550\text{ nm}$ ," *Opt. Express* **15**, 17967-17972 (2007).
12. M. Rui, I. Akira, M. Atsushi, and M. Hideki, "Low-resistivity phosphorus-doped polycrystalline silicon thin films formed by catalytic chemical vapor deposition and successive rapid thermal annealing," *J. J. Appl. Phys.* **41**, 501-506 (2002).
13. F. N. Xia, L. Sekaric, and Y. Vlasov, "Ultracompact optical buffers on a silicon chip," *Nat. Photonics* **1**, 65-71 (2007).

14. W. B. Jackson, N. M. Johnson, and D. K. Biegelsen, "Density of gap states of silicon grain boundaries determined by optical absorption," *Appl. Phys. Lett.* **43**, 195-197 (1983).
  15. R. E. Jones, Jr. and S. P. Wesolowski, "Electrical, Thermoelectric, and Optical properties of strongly degenerate polycrystalline silicon films," *J. Appl. Phys.* **56**, 1702-1706 (1984).
  16. J. S. Foresi, M. R. Black, A. M. Agarwal, and L. C. Kimerling, "Losses in polycrystalline silicon waveguides," *Appl. Phys. Lett.* **68**, 2052-2054 (1996).
  17. A. M. Agarwal, L. Liao, J. S. Foresi, M. R. Black, X. M. Duan, and L. C. Kimerling, "Low-loss polycrystalline silicon waveguides for silicon photonics," *J. Appl. Phys.* **80**, 6120-6123 (1996).
  18. L. Liao, D. R. Lim, A. M. Agarwal, X. M. Duan, K. K. Lee, and L. C. Kimerling "Optical transmission losses in polycrystalline silicon strip waveguide: effects of waveguide dimensions, thermal treatment, hydrogen passivation and wavelength," *J. Electron Mater.* **29**, 1380-1386 (2000).
  19. F. P. Payne and J. P. R. Lacey, "A Theoretical analysis of scattering loss from planar optical waveguides," *Opt. Quantum. Electron* **26**, 977-986 (1994).
- 

## 1. Introduction

Optical devices based on Silicon-on-Insulation (SOI) have become an active research and development field since the mid-80s [1]. Because the processes are compatible with complementary metal-oxide-semiconductor (CMOS) and their structures are potentially to be integrated monolithically, it is possible to realize mass production cost effectively. In parallel to the effort of integrating photonics devices on SOI substrate based on Si-wire or Si-rib waveguides, deposition prepared poly-Si, SiON or SiN have been considered as promising optical interconnect waveguides in multi-level scheme. Compared to crystal Si material, the fabrication of poly-Si material is simple and the period is very short. So, its cost is very cheap. Meanwhile, Poly-Si has some special applications. For the optical passive devices, Poly-Si is easy to fabricate multilayer devices, such as 3 dimension (3D) photonic crystals and multilayer resonator [2], with other semiconductor processes. All of SOI optical devices are based on single layer structure, and it is very difficult to design and fabricate 3D devices. For the optical active devices, Poly-Si must be used to partly take place of Si to produce a several-nanometer-wide gap in the high speed MOS optical modulator because of the etch process limitation of crystal Si [3-5]. Poly-Si thin films are used as gate or capacitor electrodes of ultra-large-scale integrated circuits and source/drain electrodes of thin-film transistors (TFTs) [6-8].  $\alpha$ -Si is another kind of Si material and also attracts the interests of researchers [9-11], except from crystal Si and Poly-Si.  $\alpha$ -Si has lower propagation loss and fabrication temperature than poly-Si, but  $\alpha$ -Si has higher electrical resistivity which seriously limits the response speed in the active device [4], [12]. However, one major challenge of using poly-Si material is its propagation loss. Compared to sub-micron-sized silicon waveguide with relatively low propagation loss (e.g.,  $\sim 1.7$ dB/cm [13]), poly-Si waveguide exhibits much higher propagation loss, which ultimately limits its application scope.

Previously, the reported loss of poly-Si is  $> 100$ s dB/cm [14-15], so it didn't receive much attention as being the waveguide material in the optical application. Some important research works have contributed to the development of low loss poly-Si waveguide [16-18]. Foresi, *et al.*, [16] reported the poly-Si loss  $\sim 34$ dB/cm at 1550nm by CMP method. Agarwal, *et al.*, [17] reported 15dB/cm of poly-Si waveguide at 1550nm by hydrogenation and Liao, *et al.*, [18] reported the lowest loss of 9dB/cm at 1550nm. All of above reports only provided the loss at 1550nm or 1310nm. Although the propagation loss of poly-Si waveguide has reduced from several hundred dB/cm to 9dB/cm, we need to further reduce the propagation loss for wide application. Meanwhile, the waveguides in above researches which widths almost are several microns are multimode waveguides. Recent research of Si-microphotonics has been pushed into the sub-micron level waveguides, so it is important to investigate the relevant optical transmission performance of poly-Si waveguides in similar dimensions.

In this work, we fabricated sub-micron size poly-Si single mode waveguides integrated with SiON waveguide coupler. We measured the propagation loss of poly-Si waveguides and the coupling loss with optical flat polarization-maintaining fiber (PMF) by cut-back technique. This fiber diameter is about  $9.0\mu\text{m}$  and directly cleaved with a cleaver. In the entire C-band, the propagation loss of TE mode is  $\sim 6.45\pm 0.3$ dB/cm and the coupling loss with

optical flat PMF is  $\sim 3.4\text{dB}/\text{facet}$ . To the best of our knowledge, the propagation loss is one of the best results among the previously reported works. We also measured the TM mode of this waveguide. The propagation loss of TM mode is  $\sim 7.11 \pm 0.5\text{dB}/\text{cm}$  and the coupling loss is more than  $6.7\text{dB}/\text{facet}$ . In section 2, we introduce the design and fabrication of the poly-Si waveguide surrounded by SiON and the SiON coupler. In section 3, we measure the optical transmission performance of poly-Si waveguides and analyze the factors, including the effect of refractive index contrast and roughness and others. Compared to the SiO<sub>2</sub> cladding in above reported papers, poly-Si waveguide with SiON cladding has the lower propagation loss.

## 2. Design and Fabrication

It is challenge to couple the sub-micron-size waveguide with optical single mode fiber (SMF). High coupling loss would cause a large measurement error and uncertainty. To this regard, we designed a SiON coupler to reduce the coupling loss, as illustrated in Fig. 1. The refractive index of SiON material is 1.51, slight higher than the refractive index (1.46) of SMF. In order to match the  $9.2\mu\text{m}$ -diameter core size of SMF, we designed the square cross-section of  $6\mu\text{m} \times 6\mu\text{m}$  SiON waveguide in the input/output of SiON coupler. A SiO<sub>2</sub> layer is used to clad the SiON waveguide, in order to protect the waveguides and the coupler from any damage in the whole processes, especially for the dicing and the polishing processes. The coupling loss of this SiON waveguide with flat SMF is  $\leq 0.2\text{dB}$  based on simulation by beam

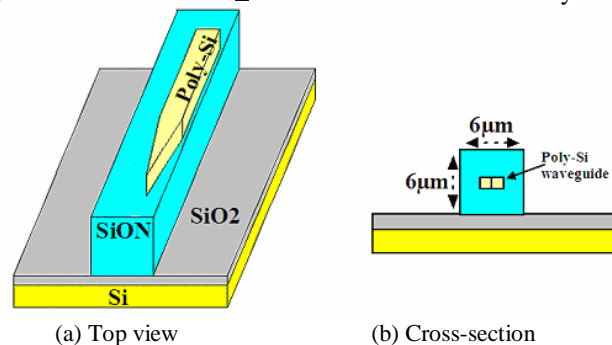


Fig. 1. Schematic diagram of the SiON coupler.

propagation method (BPM) of RSOFT software. The strip poly-Si waveguide is placed in the center of the SiON waveguide. The tip width of poly-Si waveguide in the input/output is  $150\text{nm}$  and its coupling length is  $200\mu\text{m}$ . The distance between the coupling face of SiON and the tip of Poly-Si waveguide is about  $500\mu\text{m}$ . The optical signal from optical fiber first propagates in the SiON coupler, and then gradually transferred into the poly-Si waveguide by the tip structure. Because the refractive index of poly-Si is higher than that of SiON, the structure can efficiently confine optical signal propagating in the poly-Si waveguide. In this experiment, three widths of poly-Si designed are  $300$ ,  $500$  and  $700\text{nm}$ . There are 9 waveguides with different length for each width group, in which the length was offset by  $1\text{mm}$  between neighboring waveguides. Two  $180$ -degree bend waveguides with the same diameter of  $60\mu\text{m}$  are included in each waveguide. The simulated coupling loss of this coupler with flat SMF is about  $2\text{dB}/\text{facet}$ . For this and above simulated results, we only take account of the mode-size mismatch during the simulation of coupling loss using the BPM method. This coupling loss is mainly caused by the big tip width as limited by the process capability.

In our experiment, six 8-inch-Si wafers were used, named as wafer-A to -F. A  $5000\text{\AA}$ -thick SiO<sub>2</sub> layer first was deposited on these bare Si wafers by plasma-enhanced chemical vapor deposition (PECVD). The oxide thickness of  $5000\text{\AA}$  is sufficient to reduce optical leakage from the SiON waveguide into the substrate.  $3.0\mu\text{m}$ -thick SiON layer was deposited as the bottom cladding. If the first SiO<sub>2</sub> layer is thicker than  $1\mu\text{m}$ , the cracks easily appear on the SiON layer after high temperature anneal because of the thermal stress. The atomic force

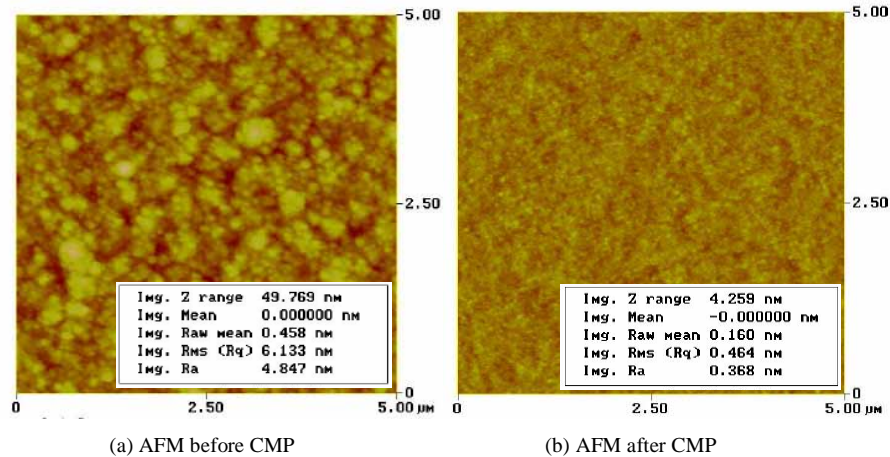


Fig. 2. AFM picture of the surface of deposited SiON layer before and after CMP process

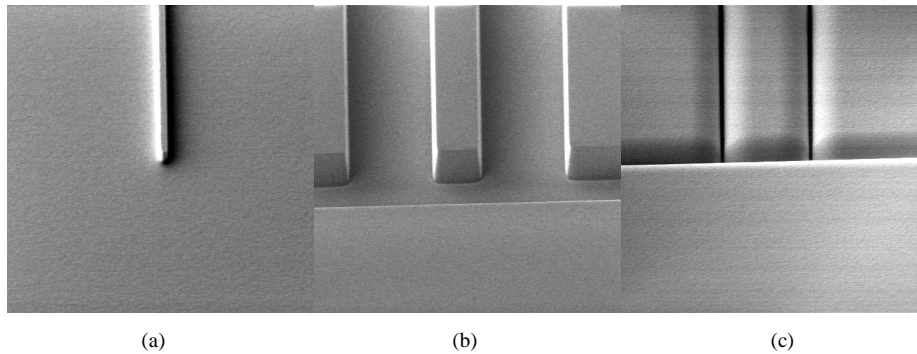
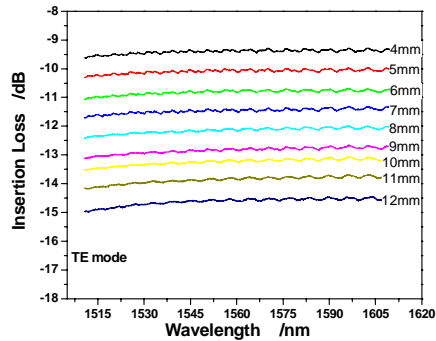


Fig. 3. SEM images of SiON coupler: (a) Tip structure of poly-Si waveguide; (b)  $6\mu\text{m}\times 6\mu\text{m}$  SiON waveguide coupler; (c) SiON waveguide covered with  $10\mu\text{m}$  SiO<sub>2</sub> cladding layer.

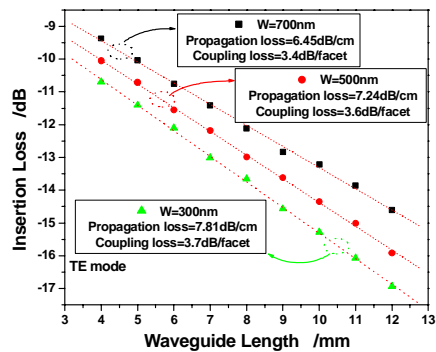
microscope (AFM) image of the SiON surface after deposition is shown in Fig. 2(a). This AFM image shows the surface of SiON is very rough. The roughness is  $\sim 6\text{nm}$ . To prevent such roughness being transferred to subsequent poly-Si layer, it is necessary to polish the surface of SiON layer. The surface of the SiON layer was polished by chemical mechanical polish (CMP), shown in Fig. 2(b). The roughness after CMP is only  $0.46\text{nm}$ . It is apparently smoother than the surface roughness ( $\sim$ several nanometers) as reported by Foresi, *et al.*, [11]. Subsequently, a  $250\text{nm}$ -thick amorphous Si layer was deposited on the wafers (A, B, C) and  $150\text{nm}$ -thick amorphous Si layer was deposited on the wafers (D, E, F) by LPCVD at  $550^\circ\text{C}$ . All samples were then annealed in N<sub>2</sub> at  $575^\circ\text{C}$  for 15 hours. A/D, B/E and C/F wafers are further annealed at  $1100^\circ\text{C}$  for 30min, 60min and 120min, respectively. The amorphous Si was annealed into poly-Si after anneal. The surfaces of poly-Si samples after anneal were inspected by AFM and the surface roughness levels are found to be maintained about  $0.4\text{nm}$ . So, it is not necessary to polish the surface of Poly-Si layer by CMP method. The waveguide structures were patterned with  $248\text{nm}$  deep UV lithography and directly etched to the SiON top surface with an ICP-RIE etch, using the resist as the etch mask. The tip structure of poly-Si waveguide is shown in Fig. 3(a). In order to further reduce the roughness,  $150\text{\AA}$ -SiO<sub>2</sub> layer was grown thermally on the surface of poly-Si. Another  $3.0\mu\text{m}$ -thick SiON layer as the upper cladding was deposited above the poly-Si waveguide. The  $6\mu\text{m}\times 6\mu\text{m}$  SiON coupler was patterned and etched after second CMP, shown in Fig. 3(b). The tip of poly-Si waveguide is in

the center of the SiON waveguide. Finally, 10 $\mu$ m low stress SiO<sub>2</sub> layer shown in Fig. 3(c) was deposited by PECVD, which protects the waveguides from damage during the subsequent processes, e.g., dicing and polish.

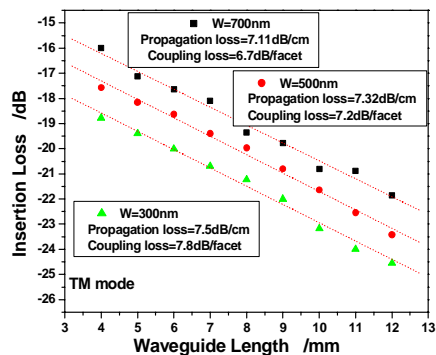
### 3. Results and Analysis



(a)



(b)



(c)

Fig. 4. Measured results of poly-Si waveguides with SiON coupler for TE mode in wafer C. (a) Measured spectrum of 700nm-wide and 250nm-high poly-Si waveguides in C-band wavelength; (b) Propagation and coupling loss of 250nm-high poly-Si waveguides for TE mode by cut-back technique at 1550nm; (c) Propagation and coupling loss of 250nm-high poly-Si waveguides for TM mode by cut-back technique at 1550nm.

The samples are first polished to reduce the coupling loss with the optical flat fiber after dicing. We use the optical flat polarization-maintaining fiber to couple the waveguides. Then, the samples are characterized by cut-back method using a high-precision tunable light source with C-band wavelength, polarization controller, polarizer and an optical high-precision power meter. In order to measure the loss of TE mode, we adjust the polarization controller and rotate the PMF holder before testing the waveguides. All of optical fibers are the PM fibers in our measurement. The spectrum results of 700nm-wide waveguides in wafer-C are shown in Fig. 4(a). The propagation loss of TE mode at 1550nm is 6.45dB/cm, and the TE mode propagation loss within the entire C-band is  $\sim 6.45 \pm 0.3$ dB/cm. The coupling loss is slight different for different wavelength, especially in the range of relative low wavelength. And the coupling loss is  $\sim 6.8 \pm 0.2$ dB within the C-band wavelength. The measured results of waveguides with different widths in wafer-C by cut-back method are shown in Fig. 4(b). The results show that the propagation loss of TE mode is reduced with the increase of waveguide width (300nm to 700nm). TM mode is also measured, shown in Fig. 4(c). The propagation loss of TM mode is more than 7.11dB/cm, and the coupling loss of TM mode is higher than TE mode, more than 6.7dB/facet. Like TE mode, the propagation loss of TM mode is also reduced with the increase of waveguide width (300nm to 700nm).

We simply analyze scattering loss ( $\alpha$ ) caused by the roughness, the width and the refractive index contrast from the following equation reported by Payne in [19]:

$$\alpha = \frac{\sigma^2}{\sqrt{2}k_0d^4n_1} g(V)f_e(x, y) \quad (1)$$

Where,  $\sigma$  is the roughness of waveguide's surface,  $k_0$  is the free-space wave number,  $d$  is the half width of waveguide,  $n_1$  is the core index.  $g(V)$  and  $f_e(x, y)$  are dependant on the waveguide parameters and the correlation length  $L_c$ . Given  $L_c$  of 50nm, we can calculate the results of 250nm-height waveguides using the Eq. (1), shown in Fig. 5. According to these results, the scattering loss is reduced with the increase of waveguide width, especially for the waveguide with rougher surface. So, the scattering loss caused by the surface can be reduced by designing wider waveguide. When the roughness is about 0.3nm, this roughness induced scattering loss is less than 0.05dB/cm. So, in our experiment, the scattering loss caused by the bottom and upper surface is completely negligible. Except from the internal scattering loss, the surface scattering loss is mainly caused by the side-wall roughness in our samples. Although thermal growth can reduce the side-wall roughness, it is limited and difficult to control for nanometer waveguides. This picture also shows that the scattering loss is dependent on the refractive index of cladding layer. The cladding layer with higher refractive index can achieve lower scattering loss caused by surface roughness.

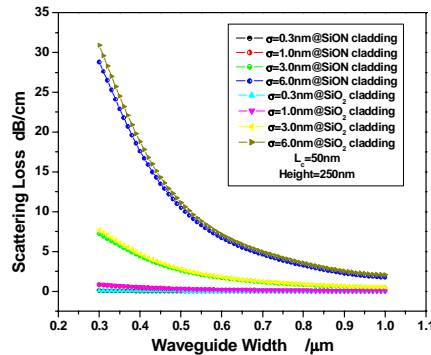


Fig. 5. Simulated scattering loss caused by surface roughness and refractive index contrast

From the TE/TM mode field distribution in the channel waveguide, the above/bottom surface roughness and the height of waveguide is more critical to the loss of TM mode than TE mode [11]; the side-wall roughness and the width of waveguide is more important to TE mode. For our waveguide ( $H=250\text{nm}$ ;  $W=700\text{nm}$ ), the loss of TM mode is close to the loss of TE mode. The result shows the side-wall is rougher than the top and bottom surfaces. We estimated that the side-wall roughness in the long range was more than  $6\text{nm}$ , according to the performance of our process. According to the calculated results in Fig. 5, the propagation loss of Poly-Si reduced more than  $1\text{dB/cm}$  after the SiON cladding took the place of  $\text{SiO}_2$  cladding because of the high side-wall roughness. So, we can minimize the loss for poly-Si waveguide clad by SiON than by  $\text{SiO}_2$ .

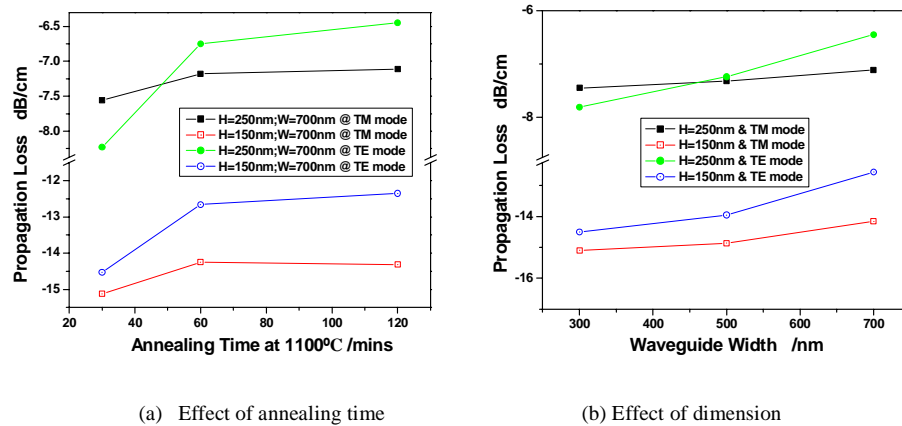


Fig. 6. Measured propagation loss of TE mode vs. annealing time and dimension of poly-Si waveguide

Compared to low-loss waveguide based on SOI, the loss of poly-Si waveguide is mainly caused by the interfacial grain boundaries. Annealing at high temperature is effective to reduce these internal scattering losses at present. The measured results of the annealed samples at  $1100^\circ\text{C}$  are shown in Fig. 6(a). Propagation loss of TE mode can be reduced more than  $1\text{dB/cm}$  by annealing at  $1100^\circ\text{C}$ , especially for thinner poly-Si waveguide. But the amplitude on the downside gradually decreases with the increase of the annealing time. So, it is not available to reduce the propagation loss by infinitely increasing the annealing time. Figure 6(a) also shows the effect of annealing time on TM mode. Short annealing time can obviously reduce the loss of TM mode, but it is difficult to reduce the loss of TM mode by longer annealing time. Figure 6(b) shows the propagation loss of poly-Si waveguide with different height for both TE mode and TM mode. The height of waveguide affects obviously the propagation loss. The interaction between the optical signal and the surface of waveguide is stronger in thinner waveguide than in thicker waveguide. So, the propagation loss performance in thinner waveguide is more sensitive to the roughness of the surface and the interfacial scattering.

#### 4. Conclusion

A low-loss Sub-Micron polycrystalline silicon waveguide clad by SiON with effective coupler has been presented. The measured results show the propagation losses of TE/TM modes are  $\sim 6.45 \pm 0.3 \text{ dB/cm}$  and  $7.11 \pm 0.5 \text{ dB/cm}$  in the whole C-band wavelength, respectively. The coupling loss with optical flat polarization-maintaining fiber (PMF) is about  $3.4 \text{ dB/facet}$  for TE mode, but the coupling loss for TM mode is high. The cladding layer with higher refractive index can achieve lower scattering loss caused by surface roughness. So, we can get lower loss poly-Si waveguide clad by SiON than by  $\text{SiO}_2$ . Compared to former reported results, it is the lowest propagation loss of poly-Si waveguide.